Letter Vol. 50, No. 20/15 October 2025/*Optics Letters* 6369

Optics Letters

Bismuth-doped fiber amplifier for full S-band amplification

Aleksandr Donodin,[1,*] **Vitaly Mikhailov,**[2] **Jiawei Luo,**[2] **Dmitrii Stoliarov,**[1] **David J. DiGiovanni,**[2] **and Sergei K. Turitsyn**[1]

[1]*Aston Institute of Photonic Technologies, Aston University, B4 7ET Birmingham, UK*
[2]*OFS Laboratories, 19 Schoolhouse Rd., Somerset, New Jersey 08873, USA*
**a.donodin@aston.ac.uk*

Received 31 July 2025; revised 11 September 2025; accepted 16 September 2025; posted 17 September 2025; published 13 October 2025

We report the first single-stage/single-pass bismuth-doped fiber amplifier (BDFA) achieving > 10 dB gain across the full S-band (1465–1530 nm), a critical step toward extending capacity in multi-band optical transmission systems. The proposed amplifier employs a 400 m-long germanosilicate fiber, bi-directionally pumped at 1425 nm, delivering 11.3–35.6 dB small-signal gain and a noise figure of 5.6–7.7 dB. Compared to thulium- and Raman-based S-band solutions, our BDFA offers a compact, efficient, and silica-compatible platform with improved performance in the lower S-band, where other technologies struggle. This demonstration paves the way for practical S-band amplification in future high-capacity, power-efficient optical networks without reliance on fluoride fibers or kilometer-scale nonlinear media.

https://doi.org/10.1364/OL.575125

Introduction. Multi-band transmission (MBT) is one of the most attractive short- to mid-term solutions for addressing the relentless growth in internet capacity demand [1,2]. Currently, C- and L-band links utilize only 12 THz of the approximately 60 THz available for data transmission within the low-loss bandwidth of single-mode fiber (SMF) [3]. Naturally, the S-band—spectrally adjacent to the C-band—has attracted significant attention for extending C + L systems, due to its relatively low loss, manageable dispersion, and broad 9 THz bandwidth. Recently, numerous demonstrations of S+C+L systems [4,5] and MBT systems involving S-, C-, and L-bands [6–8] have highlighted the excellent potential of S+C+L transmission as a viable short- to medium-term strategy for capacity expansion.

Expanding into the S-band not only enables the use of an additional 9 THz of optical spectrum but also provides spectral continuity that simplifies the design of transceivers and multiplexing components. From a practical perspective, utilizing the S-band allows existing fiber infrastructure to support significantly higher aggregate capacities without the need for costly fiber deployments or disruptive overbuilds. However, the successful implementation of S-band transmission hinges critically on the availability of high-performance optical amplifiers that can operate efficiently in this spectral region.

Despite the great success of S+C+L-band MBT, amplification solutions within the S-band remain limited. To date, two main candidates for S-band amplification have been considered: thulium-doped fiber amplifiers (TDFAs) and Raman amplifiers [9]. TDFAs are typically based on fluoride glass, which restricts their performance in terms of both gain and noise figure (NF), and also present challenges in fiber handling [10,11]. Distributed Raman amplifiers offer excellent performance, particularly over long distances; however, they are insufficient for coherent systems and require complementary lumped amplification technologies [12]. Lumped Raman amplifiers can match the performance of TDFAs [12], but rely on specialized nonlinear fibers with lengths up to 10 km. This makes them impractical for compact or cost-sensitive systems. Other amplification technologies include semiconductor optical amplifiers [13] and fiber optic parametric amplifiers [14], each with inherent limitations and limited investigation in the S-band. SOAs often suffer from high noise figures (NF) and limited gain flatness, while parametric amplifiers require precise phase matching and typically operate over narrower bandwidths and require high pump powers (>1 W) [14].

Another promising candidate is the bismuth-doped fiber amplifier (BDFA), which has drawn increasing attention for its capability to amplify across a wide wavelength range, including the O-, E-, S-, and U-bands [15]. BDFAs are based on silica-compatible glass hosts, which makes them attractive for integration into existing fiber systems without the mechanical fragility and splicing issues of fluoride fibers. Furthermore, their potential for compact, high-efficiency designs makes them well-suited for access networks, regional links, and data center interconnects. However, BDFAs have so far demonstrated limited performance in the S-band, typically reaching up to 1500 nm [16,17]. A recent dual-stage BDFA design extended amplification into the S-band, but still showed limited performance while utilizing pump wavelengths around 1320 nm [18]. Recent work has systematically compared single- and double-pass BDFA configurations for S-band operation [19]. It reports that a single-pass BDFA with an ~200 m active fiber does not provide sufficient gain to span the full S-band at small-signal inputs (e.g., −30 dBm), whereas introducing a second pass increases

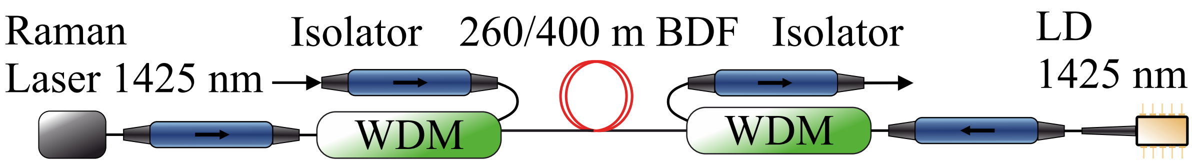

Fig. 1. Schematic of the bidirectionally pumped BDFA.

the effective interaction length and boosts gain (to ~42–43 dB over 1460–1540 nm), albeit with a penalty in noise figure (6.3–11 dB) and added complexity/loss. This suggests that the full potential of BDFAs in the S-band has yet to be realized and that further development is required to unlock their capability across the entire 1465–1530 nm window.

In this work, we propose a novel alternative design of a BDFA targeting S-band amplification using a long pump wavelength of 1425 nm along with a 400 m-long germanosilicate bismuth-doped fiber to achieve a high small-signal gain of 11.3–35.6 dB with an NF of 5.6–7.7 dB across the full S-band (1465–1530 nm). To the best of our knowledge, this is the first demonstration of a silica-based single-stage/single-pass BDFA capable of delivering >10 dB gain throughout the entire S-band, representing a critical advancement toward practical, multi-band amplification solutions for next-generation optical networks.

Amplifier characterization. The experimental setup of the developed S-band BDFA is shown in Fig. 1. The amplifier features a conventional bi-directionally pumped BDFA structure comprising two signal isolators at 1500 nm, two pump isolators at 1430 nm, and a pair of thin-film filter wavelength division multiplexers (TFF-WDMs) with a 1260–1457.5 nm pass band and a 1464.5–1620 nm reflection band. A 250 mW pump laser at 1425 nm was used for forward pumping, while a tunable Raman laser operating in the 1435–1465 nm range was employed for backward pumping. The active fiber was a germanosilicate bismuth-doped fiber tested in two lengths: 260 m (Case 1) and 400 m (Case 2). The fiber had a GeO_2 concentration of approximately 14 mol%, a step-index design, and a core numerical aperture (NA) of 0.21. The mode field diameter is 6 µm at 1550 nm. Two fiber lengths were tested: 260 m and 400 m. Gain, NF, and power conversion efficiency (PCE) were measured using the experimental setup and methodology previously developed for E-band BDFA characterization [20], across the 1460–1530 nm spectral range. Characterization was carried out at two input signal power levels: 0 dBm and −20 dBm. The laser diode pump power was fixed at 250 mW, and the Raman laser was set to 700 mW, giving a total pump power of 950 mW. The Raman laser wavelength was fixed at 1425 nm, as increasing the wavelength led to degraded amplifier performance.

We first characterized the amplifier using a 260-m-long BDF and a fixed forward pump power of 250 mW. The results are shown in Fig. 2. The measured wavelength range was limited to 1465–1505 nm. The amplifier delivered a peak small-signal gain of 24.5 dB at 1465 nm, which smoothly decreased to 11.5 dB at 1505 nm. The corresponding NF ranged from 5.6 dB to 7.2 dB. For a 0 dBm input signal, the amplifier exhibited a peak gain of 16.5 dB at 1465 nm and 10.6 dB at 1505 nm, with NF values between 6 and 8.9 dB. A summary of the achieved amplifier parameters is presented in Table 1. Performance for this configuration was recorded using only forward pumping at 250 mW, as increasing the pump power did not significantly enhance the gain

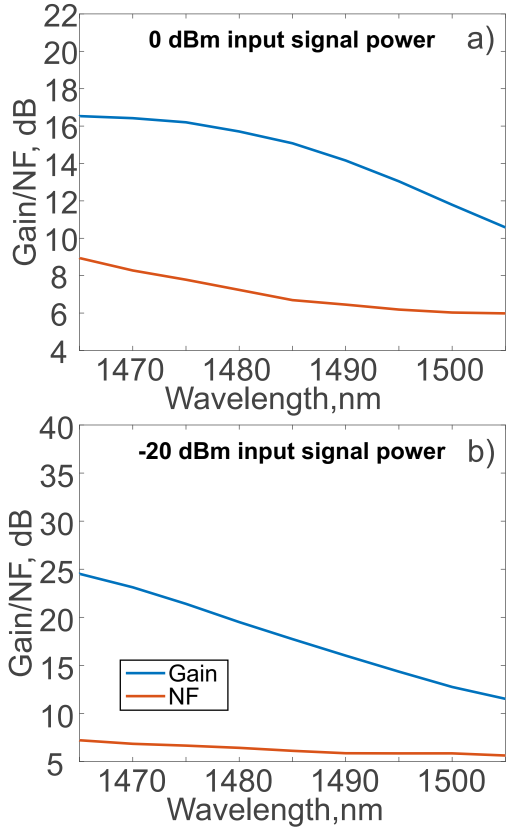

Fig. 2. Gain and NF of 260 m-long BDFA with 250 mW pump power for (a) 0 dBm and (b) −20 dBm input power.

in the longer-wavelength region of the S-band (yielding less than 1 dB improvement in small-signal gain despite an additional 700 mW of pump power).

To further investigate the amplifier and improve its performance within the S-band, we increased the length of the active BDF to 400 m. In this case, the operation of the BDFA was recorded over a broader wavelength range of 1465–1530 nm. As a first step, the amplifier was tested with only 250 mW of backward pump power; the recorded gain and NF are presented in Figs. 3(a) and 3(b). It can be seen that the gain is higher for small signal amplification compared to the 260 m case, with a maximum gain of 32 dB at 1465 nm for an input signal power of −20 dBm. However, the NF is significantly higher than in the 260 m case, reaching 17 dB for 0 dBm input signal power and 10 dB for small signal amplification. The gain ranges from 8.6 dB to 16.1 dB and from 9.4 dB to 31.5 dB for 0 dBm and −20 dBm input powers, respectively. The NF, on the other hand, varies from 6.6 dB to 16 dB and from 6.2 dB to 10.1 dB. This degradation in performance can be attributed to insufficient pumping, which leaves the beginning of the fiber significantly underpumped. As a result, especially at shorter wave-

Table 1. Main BDFA Characteristics for Different Pumping Schemes and Two Levels of Input Signal Powers: 0 dBm and −20 dBm[a]

Amplifier Scheme (BDF Length–Pump Power)	Gain (dB) 0 dBm	−20 dBm	NF (dB) 0 dBm	−20 dBm	PCE (%) 0 dBm	−20 dBm
260 m–250 mW	10.6–16.5	11.5–24.5	6–8.9	5.6–7.2	18	1.1
400 m–250 mW	8.6–16.1	9.4–31.5	6.6–16	6.2–10.1	16.3	5.6
400 m–700 mW	10.2–18.1	10.9–33.1	5.9–7.8	5.7–8.6	9	3
400 m–950 mW	10.6–21.2	11.3–35.6	5.9–7.8	5.6–7.7	13.9	3.8

[a]Ranges are indicated for the wavelength band of 1465–1505 nm for 260 m–250 mW and 1465–1530 nm for all 400 m schemes.

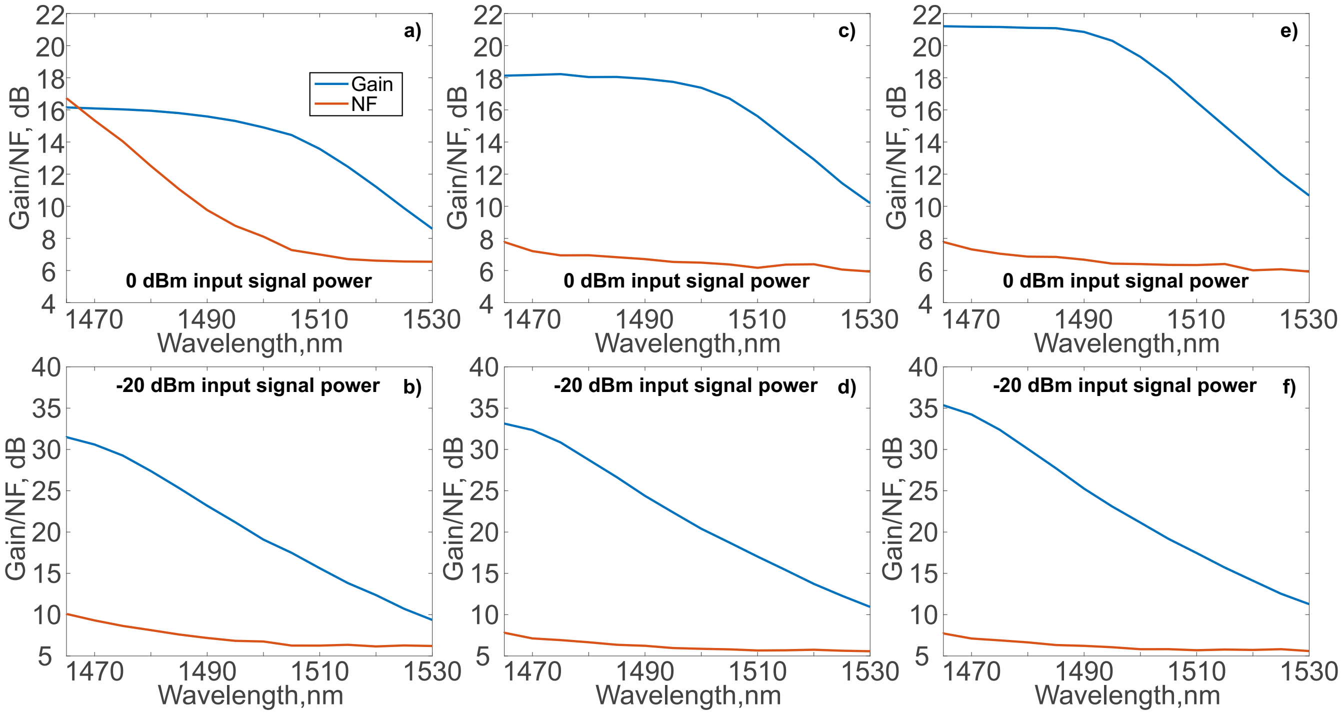

Fig. 3. Gain and NF for 400 m-long BDFA with 250 mW pump power for (a) 0 dBm and (b) −20 dBm input power; 700 mW pump power for (c) 0 dBm and (d) −20 dBm input power; 950 mW pump power for (e) 0 dBm and (f) −20 dBm input power.

lengths below 1505 nm, the absorption cross section continues to dominate, leading to increased losses.

To address this, the pump power was increased to 700 mW using only forward pumping (Raman laser at 1425 nm). The results are shown in Figs. 3(c) and 3(d). This change led to significant improvements in both gain and NF for both input signal powers. The NF achieved ranges from 5.9 dB to 7.8 dB for 0 dBm input, and from 5.6 dB to 7.8 dB for −20 dBm input, achieving better results at 0 dBm than the shorter amplifier. The gain spans 10.2–18.1 dB for 0 dBm input and 10.9–33.1 dB for −20 dBm input. Notably, increasing the pump power and amplifier length significantly enhanced performance in the longer wavelength range, reaching similar gain at 1530 nm as the 260 m-long amplifier achieved at 1505 nm. The 3-dB gain bandwidth in this configuration extends from 1465 to 1512 nm—the widest among all tested setups.

Finally, both forward and backward pumps were used, totaling 950 mW of pump power. The corresponding gain and NF are presented in Figs. 3(e)–3(f). This configuration of the 400 m-long amplifier achieved the highest gain across both input powers: 10.6–21.2 dB for 0 dBm, and 11.3–35.6 dB for −20 dBm. The NF is similar to that observed with 700 mW forward pumping and is summarized in Table 1. It is important to note that this pumping configuration enabled significantly higher gain at longer wavelengths than the 260 m configuration. Specifically, the 3-dB gain bandwidth for 0 dBm input is 1465–1505 nm, achieving 18.2 dB at 1505 nm, which is 7.6 dB higher than the gain at the same wavelength in the 260 m case. For small signal amplification, the amplifier delivers a gain > 20 dB in the spectral range of 1465–1502.5 nm. This demonstrates that the developed amplifier provides sufficient gain to cover the lower part of the S-band, where TDFAs typically struggle to offer both adequate gain and low NF. In terms of NF, the amplifier exhibits a gradually improving profile toward shorter wavelengths, maintaining values between 5.6 and 7.9 dB across the entire spectral range for all input powers.

As the final step, the PCE of the amplifiers is compared. The highest PCE for 0 dBm input signal power is achieved in the 260 m-long scheme with 250 mW of pump power, reaching 18%. However, this scheme exhibits relatively low PCE for small signal amplification due to its modest gain. The best PCE for small signal amplification is observed in the 400 m-long scheme with low pump power, reaching 5.6% at 250 mW pump power, which can be attributed to more efficient pump absorption in the longer fiber. Bi-directional pumping at a maximum of 950 mW pump power allows to achieving 13.9 % PCE for 0 dBm input signal power and 3.8 % for −20 dBm input signal power.

Beyond PCE, the 400 m-long BDFA with 950 mW of total pump power demonstrates the best overall performance in terms of gain and achievable bandwidth. Nevertheless, the amplifier NF remains subject to further optimization. As previously demonstrated [18,20], NF below 5 dB is achievable in the S-band with lower-wavelength pumps. Therefore, a combination of low- and high-wavelength pumping may offer a viable strategy to simultaneously achieve low NF and sufficient gain across the S-band. The maximum achievable small signal gain exceeds 35 dB for 950 mW pump power, and exceeds 21 dB in the saturated regime with input signal power of 0 dBm. The amplifier features 20 > dB small signal gain for the range of 1460–1505 nm.

We benchmark our single-pass, single-stage/pass BDFA against recent S-band reports. Wang et al. [19] use 1310 nm pumping in a *double-pass* BDFA and report peak S-band gain of ≈42.8 dB with NF of 6.3–11 dB over 1460–1540 nm at a small-signal input of −30 dBm. By contrast, our amplifier has a simpler single-pass architecture and achieves a lower NF of 5.6–7.7 dB at a higher input power (−20 dBm), while still providing 11.3–35.6 dB gain across 1465–1530 nm. The cascaded BDF+EDF hybrid of Qi *et al.* [21] delivers broadband E +S+C+L operation and, in the S-band, > 29.5 dB gain with NF < 6.5 dB at −30 dBm using a dual-stage design (200 m BDF pumped at 1310 nm plus 4 m EDF pumped at 980 nm). In contrast, our approach employs a single BDF stage with a longer-wavelength pump at 1425 nm, reducing component count and inter-stage loss while ensuring efficient pump absorption via a longer active fiber. To our knowledge, this is the first demonstration of a single-stage/pass BDFA capable of providing consistent and reasonable gain (> 10 dB) across the entire S-band for both small-signal and 0 dBm input signal power amplification.

Conclusions. We have, for the first time, demonstrated a bismuth-doped fiber (BDF-only) S-band amplifier that delivers greater than 10 dB of gain across the entire S-band (1465–1530 nm) for both −20 dBm and 0 dBm input signal powers. The amplifier achieves a high small-signal gain of 11.3–35.6 dB with a noise figure in the range of 5.6–7.9 dB across the full spectral band. This performance is achieved using a 400 m-long germanosilicate BDF pumped at 1425 nm, without the need for fluoride-glass components (like in TDFAs) or kilometer-scale nonlinear media (like in DRA).

Compared to existing S-band amplification technologies—such as TDFAs, Raman amplifiers, our BDFA offers a compact, silica-compatible, and energy-efficient alternative, particularly in the lower S-band, where other technologies typically exhibit reduced gain or elevated noise figures. The demonstration shows a great promise for BDFAs to be deployed in multi-band coherent systems.

Funding. Engineering and Physical Sciences Research Council (EP/R035342/1, EP/W002868/1); Royal Academy of Engineering (Research Fellowship); Department for Science, Innovation and Technology.

Acknowledgment. This work was supported by UK EPSRC grant TRANSNET (EP/R035342/1) and Advanced Optical Frequency Comb Technologies and Applications (EP/W002868/1), the Department of Science and Innovation and Technology, and the Royal Academy of Engineering under Research Fellowship.

Disclosures. The authors declare no conflicts of interest.

Data availability. Data underlying the results presented in this paper is available upon reasonable request.

REFERENCES

1. A. Ferrari, A. Napoli, J. K. Fischer, *et al.*, J. Light. Technol. **38**, 4279 (2020).
2. P. J. Winzer, D. T. Neilson, and A. R. Chraplyvy, Opt. Express **26**, 24190 (2018).
3. T. Hoshida, V. Curri, L. Galdino, *et al.*, Proc. IEEE **110**, 1725 (2022).
4. B. Puttnam, G. Rademacher, R. Luis, *et al.*, in *Photonic Networks and Devices* (Optica Publishing Group, 2023), p. NeTu3B–2.
5. J. Yang, H. Buglia, M. Jarmolovičius, *et al.*, J. Light. Technol. **43**, 1893 (2025).
6. B. J. Puttnam, R. S. Luis, I. Phillips, *et al.*, in *Optical Fiber Communication Conference* (2024), p. Th4A.3.
7. D. Soma, T. Kato, S. Beppu, *et al.*, *in 49th European Conference on Optical Communications (ECOC 2023)* (IET, 2023), p. 1658.
8. B. J. Puttnam, R. S. Luís, I. Phillips, *et al.*, J. Light. Technol., https://ieeexplore.ieee.org/document/10891718.
9. P. Hazarika, M. Tan, A. Donodin, *et al.*, Opt. Lett. **47**, 6472 (2022).
10. S. D. Emami, S. W. Harun, F. Abd-Rahman, *et al.*, Prog. Electromagn. Res. **14**, 431 (2009).
11. L. Rapp and M. Eiselt, J. Light. Technol. **40**, 1579 (2021).
12. D. Pratiwi, P. Hazarika, M. Tan, *et al.*, in *Laser Science* (Optica Publishing Group, 2024), p. JW5A–8.
13. J. Renaudier, A. Arnould, A. Ghazisaeidi, *et al.*, J. Light. Technol. **38**, 1071 (2020).
14. C. B. Gaur, V. Gordienko, P. Hazarika, *et al.*, in *Optical Fiber Communication Conference* (Optica Publishing Group, 2022), p. W4J–1.
15. A. Donodin, in *2024 Asia Communications and Photonics Conference (ACP) and International Conference on Information Photonics and Optical Communications (IPOC)* (IEEE, 2024), p. 1.
16. A. Donodin, V. Dvoyrin, E. Manuylovich, *et al.*, Opt. Mater. Express **11**, 127 (2021).
17. V. Dvoyrin, V. M. Mashinsky, and S. Turitsyn, in *Optical Fiber Communication Conference* (Optica Publishing Group, 2020), p. W1C–5.
18. S. Noor, A. Donodin, S. Turitsyn, *et al.*, in *Optical Fiber Communication Conference* (2025), p. Tu3E.3.
19. D. Wang, J. Qi, X. Huang, *et al.*, Opt. Express **33**, 17858 (2025).
20. A. Donodin, E. Manuylovich, V. Dvoyrin, *et al.*, APL Photonics **9**, 046102 (2024).
21. J. Qi, Z. Liao, J. Zheng, *et al.*, Opt. Laser Technol. **192**, 113758 (2025).